IEEE Access
Multidisciplinary | Rapid Review | Open Access Journal

Received December 7, 2020, accepted December 12, 2020, date of publication December 23, 2020, date of current version January 6, 2021.

Digital Object Identifier 10.1109/ACCESS.2020.3046789

Transient Roebel Bar Force Calculation in Large Salient-Pole Synchronous Machines

MARIUS WENZEL MEISWINKEL, AMIR EBRAHIMI, CONSTANTIN WOHLERS, AND TIM NESCHITSCH

Institute for Drive Systems and Power Electronics, Leibniz University Hannover, 30167 Hannover, Germany

Corresponding author: Amir Ebrahimi (ebrahimi@ial.uni-hannover.de)

ABSTRACT The radial and tangential force components acting on each sub-conductor of a Roebel bar in a large generator lead to mechanical vibration of the stator bars in the slot. This double-frequency vibration results in additional mechanical stress on fixation materials in the slot and causes insulation deterioration and looseness of stator bars. Particularly during short circuits, the stator bars are subjected to immense radial forces. Understanding the origin of these vibrations and developing models to anticipate them is essential to increase the reliability and expected life time of large generators. This paper presents an analytical method for the estimation of Roebel bar forces during symmetrical and asymmetrical short circuits. For this purpose, an analytical calculation method is developed to estimate the transient three-phase currents during different short circuits. These currents induce tangential and radial flux density components along the slot width and length, respectively. An analytical approach is introduced to estimate these flux densities as a function of the slot length. Subsequently, an analytical method for calculating the Roebel bar forces considering three-dimensional transpositions is developed and verified with finite element calculations. Beyond the state of the art, the impact of the rotor field on the radial and tangential components of the stray fluxes are analytically estimated. The result is a comprehensive analytical tool for the estimation of Roebel bar forces during different short circuits in large generators.

INDEX TERMS Roebel bar forces, hydrogenerators, Lorentz force, salient-pole synchronous machines, short circuits, transient model of large generators.

I. INTRODUCTION

Studying large electrical machines is an ongoing important topic due to the various kinds of electromagnetic phenomena and modeling uncertainties caused by their immense dimensions. Despite decades spent developing calculation methods for generators in the megawatt range, there are still numerous problems and aspects to be studied [1]. The need for deepening our understanding of operational characteristics of large generators can be described considering design and operational challenges of these systems. Regarding design aspects, a more comprehensive model results in a better design with more opportunities for optimization. Regarding reliability, an extensive model describes the multi-physical relations between several parameters in a more sophisticated way and results in more deterministic life time models and improves the maintenance management, thus reducing outages and costs. Roebel bar forces are a suitable example to explain this fact. The slot stray fluxes generate double-frequency radial and tangential forces on the Roebel bars in large generators. These vibrations could lead to bar deformation, deterioration of isolation and fixation materials in the slot and in the worst case it results in sub-conductor or conductor short circuits toward the stator core or between each other. A comprehensive model of Roebel bar forces helps to understand the behavior of these forces for a better design of slot materials and a sophisticated anticipation of Roebel bar conditions.

However, since the Robel bar forces are less than the radial forces acting on the stator core and teeth, they are not comprehensively considered in the literature. In general, a simplified calculation based on the Lorenz force formulation is given for the slot ground force estimation and the tangential force on the slot wall is usually neglected. Grabner *et al.* gives an analytical approximation of displacement of Roebel bar and mechanical stress in the slot of large generators [2], [3]. Pantelyat *et al.* investigates the forces on the slot wedges [4].

The associate editor coordinating the review of this manuscript and approving it for publication was Dwarkadas Pralhaddas Kothari.

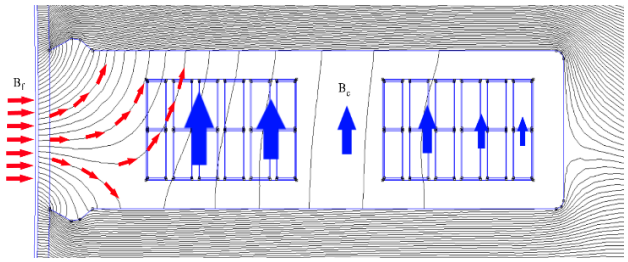

FIGURE 1. Flux lines in the slot: B_f (in red) originates from the rotor winding and B_c (in blue) from the stator winding (Roebel bar).

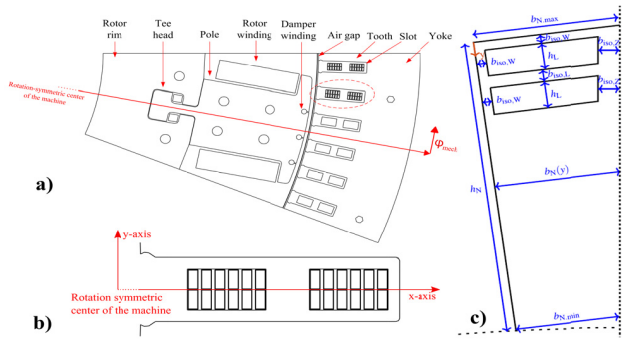

FIGURE 2. The schematic of a hydrogenerator a) one pole, b) one slot, c) half a slot with a non-constant width.

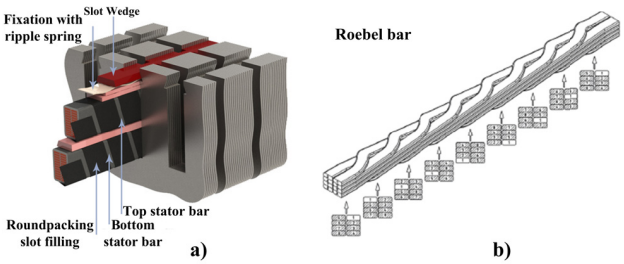

FIGURE 3. A schematic of the Roebel bar in the slot; a) upper and lower Roebel bar and bar fixations, b) transpositions of the sub-conductors in the z-direction.

The radial force acting on the slot ground mainly originates from the conductor currents and is bigger than the tangential force acting on the slot wall. However, the underlying mechanism of the tangential force is more complicated, since the rotor field is a major contributive component in the formation of tangential forces. Consequently, this force depends on the load angle, power factor, shape of the salient pole, etc. Besides, the transposition of the Roebel bar along the axial axis of the generator requires a three-dimensional consideration of the whole problem.

The estimation tool analytically calculates the transient radial and tangential force distributions on each sub-conductor along the length axis of the generator considering 3D transpositions for all rotor positions. In the first section, an investigation on the tangential and radial Roebel bar forces considering bar transposition is proposed. After that, a method for calculating the symmetrical and asymmetrical short-circuit currents is given. In the following section, an analytical tool for calculating the transverse and radial stray fluxes is proposed. In the next section, the radial forces acting on each sub-conductor and the total force acting on the whole Roebel bar are calculated and the results are numerically verified.

II. ORIGIN OF THE ROEBEL BAR FORCES

Without losing the generality of the investigation, the analysis of the Roebel bar forces is carried out for large salient-pole synchronous generators, mainly the hydrogenerators. The conductor (Roebel bar) in the slot generates fluxes across the slot with a dense concentration at the slot opening. Besides, a small portion of the air gap flux lines first enters the slot radially and then enters into the tooth tangentially. These two flux densities are responsible for the radial and tangential forces on each sub-conductor in a Roebel bar and are indicated in Figure 1. Alternating current creates an alternating flux in the conductor material and causes a skin effect. To reduce the eddy current losses in the conductors, the conductors are divided into sub-conductors, which are just connected together at the beginning and the end of the Roebel bar. To eliminate the circulating currents in the sub-conductors, every parallel-connected sub-conductor has to be surrounded exactly by the same amount of slot stray flux [5]. This is done by transposing the sub-conductors. The schematic of one pole of a hydrogenerator is indicated in Figure 2-a. Besides the pole body, the fixation, the excitation, the winding, the rotor rim and the start yoke, a stator slot is also shown in Figure 2-b and parameterized in Figure 2-c. A schematic of the Roebel bar is illustrated in Figure 3. As it can be observed, each sub-conductor experiences the position of all other sub-conductors by traveling along the generator length (Figure 3-b). The tangential (y-direction) and radial (x-direction) stray flux densities in the slot generate radial and tangential forces on the current-conducting Roebel bar acting on the slot ground and slot wall, respectively. The formulation of the Lorentz force describes these forces.

III. FLUX DENSITY DISTRIBUTION IN THE SLOT

Since the Roebel bar forces originate from the radial and tangential components of the flux density in the slot B_x and B_y, the distribution of these flux densities is described in this chapter. B_x and B_y originate from the rotor winding indicated as B_f, and from the Roebel bar located in the slot indicated as B_c in Figure 1. Therefore, the tangential and radial flux densities in the slot can be expressed by:

$$\begin{bmatrix} B_y \\ B_x \end{bmatrix} = \begin{bmatrix} B_{c,y} \\ B_{c,x} \end{bmatrix} + \begin{bmatrix} B_{f,y} \\ B_{f,x} \end{bmatrix} \tag{1}$$

These main flux components are described in the next sections.

A. RADIAL FLUX DISTRIBUTION IN THE SLOT

The radial flux density in the slot B_x, shown in Figure 4, originates from two main components. While the impact of the stator current resulting in a radial flux density $B_{c,x}$ on the sum of B_x is small and mainly present in the isolation between

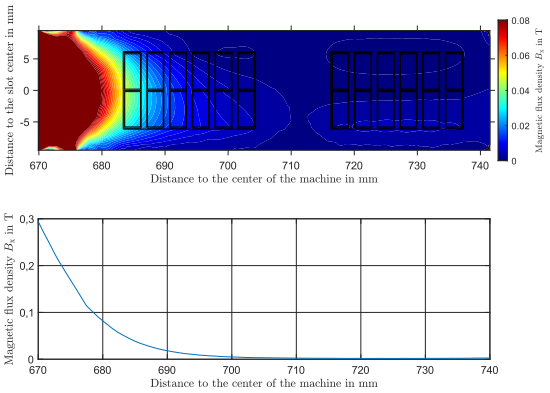

FIGURE 4. Radial component of the flux density along the slot length.

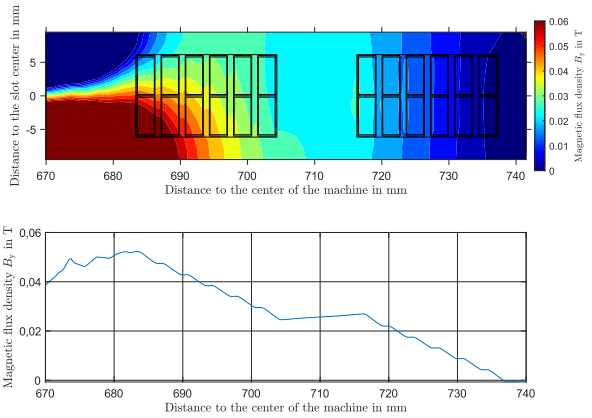

FIGURE 5. Tangential component of the flux density in the slot.

the conductors and the slot walls, the impact of the flux density originated from the rotor current $B_{f,x}$ is much more significant. Because $B_{f,x}$ originates from the moving rotor, it is conceivable that the radial flux density is a function of the rotor position and varies for different load angles and power factors (see Figure 6). The flux enters the slot from the air gap mostly in radial direction. When following the flux lines shown in Figure 1 and the flux density shown in Figure 4, it is possible to make the following assumptions:

1. The flux density in the slot is much smaller than in the teeth next to the slot,
2. The center of the largest radial flux is dependent on the position of the center of the pole,
3. The flux distributed by the rotor current mostly passes through the top Roebel bar,
4. The conductors have only a small impact on the radial flux passing them.

Because of the much larger magnetic reluctance of the slot compared to the tooth, the flux lines bend into the slot walls, resulting in an exponential decrease of B_x when traveling deeper into the slot (see equation 13).

B. TANGENTIAL FLUX DENSITY DISTRIBUTION IN THE SLOT

The tangential flux density distribution in the slot B_y also partly originates from the stator current resulting in $B_{c,y}$ and the field current resulting in $B_{f,y}$. The sum of the two components is indicated in Figure 5.

The magnetic flux density of the transverse field originated from the stator current in the slot $B_{c,y}$, can be determined by introducing the slot width gradient according to Figure 2-c:

$$b' = \frac{b_{N,min} - b_{N,max}}{h_N}, \tag{2}$$

which describes the width of the slot along the slot length by considering a trapezoidal slot shape.

$B_{c,y}$ can be estimated by dividing the MMF over the length of the stray flux in the slot (see equation 6):

$$B_{c,y}(x) = \mu_0 \frac{w_s i_L y \left(b'y + 2b_{N,max}\right)}{h_N \left(b'y + b_{N,max}\right)\left(b'h_N + 2b_{N,max}\right)}, \tag{3}$$

where i_L and w_s are the current and number of sub-conductors in the slot. However, the sub-conductors of a Roebel bar are installed in the slot discretely (see Figure 2-c). This can be considered by discretizing, the MMF:

$$\Theta_N(x) = \begin{cases} 0 & 0 < x < b_{iso,W} \\ i_L(k-1+\dfrac{A_L(x)}{A_{Lk,ges}}) & h_{L,0}(k) < x < h_{L,1}(k) \\ ki_L & h_{L,1}(k) < x < h_{L,1}(k) + b_{iso,L} \end{cases} \tag{4}$$

with the parameters indicated in Figure 2-c:

$$\begin{aligned} h_{L,0}(k) &= b_{iso,W} + (k-1)h_L + (k-1)b_{iso,L} \\ h_{L,1}(k) &= b_{iso,W} + kh_L + (k-1)b_{iso,L} \\ & \qquad k = 1, 2, \ldots, w_{sp}, \end{aligned} \tag{5}$$

which then results in the step-like MMF and flux density in the slot. For the region over and under the sub-conductor, the MMF remains constant. In the region of the sub-conductor, the MMF increases with the increasing area of the sub-conductors ($A_L(x)$). This behavior is modeled using equation 4. The magnetic flux density can be estimated with:

$$B_{c,y}(x) = \mu_0 \frac{\Theta_N(x)}{b_N(x)} \tag{6}$$

While the $B_{c,y}$ is negligible on the slot bottom, it rises linearly in every area with a sub-conductor, so that a stair-shaped flux density distribution, as indicated in Figure 5, emerges in the slot. It is constant over the tangential cross-section of the slot resulting in a maximum of flux at the upper sub-conductor. On the other hand, there is an amount of rotor flux density $B_{f,y}$ entering the slot, which is highly dependent on the position of the pole, the power factor, and the saturation of the teeth which is indicated in Figure 6. The slot ground force F_x is estimated for two full rotations (90° mechanical and 720° electrical angle for a 16-pole hydrogenerator of Figure 2-a).

Because of the relationship between the magnetic reluctance of the slot insulation and the teeth and the bending of the rotor-distributed flux into the teeth, the tangential flux density

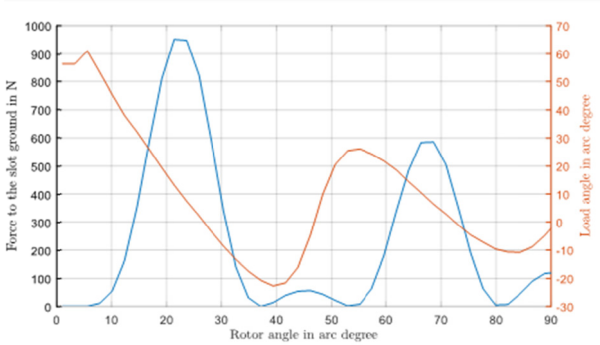

FIGURE 6. Dependency of the Roebel bar forces on the load angle and the rotor position.

at the slot walls is more influenced by the rotor flux density $B_{f,y}$ than in the center of the slot.

Every pole passes the slot at synchronous speed, and hence, the direction of the flux lines in the slot and also the direction of the current in the bars alternate with the terminal frequency. Supposing a sinusoidal function of the current over time, since the stray flux density in the slot originates from this current according to equation 6, the stray flux density is also a sinusoidal function. Therefore, the multiplication of these two parameters (according to Lorentz force formulation stated in equation 17) results in a $\cos^2(\omega t)$ function, which results in a double-frequency force on the Roebel bar acting on the slot ground.

C. IMPACT OF FIELD AND STATOR CURRENT ON THE FLUX DENSITY DISTRIBUTION IN THE SLOT

The field current is mainly responsible for generating B_x. This can be observed in Figure 4 where the exponential decrease of flux density is indicated. More interesting is the rotor-dependent behavior of B_y. The increase in the flux density at high currents can be explained by the stator core saturation.

In this case, the teeth are saturated and the difference between the slot and tooth reluctance is less, so that more flux enters the slot.

D. IMPACT OF SUB-CONDUCTOR TRANSPOSITION

To account for the stated highly uneven flux distribution in the slot, the sub-conductors in a Roebel bar transpose over the length of the core to minimize the skin effect. The path of one sub-conductor along the longitudinal axis is shown in Figure 7-b. The changing position of the sub-conductor results in a variable flux passing through them dependent on the position in the slot. If the cooling ducts in the stator core and the edge effects are neglected, it is possible to assume a constant flux over the axial length of the stator core throughout total length. If the Roebel bar is symmetrical, it is possible to approximate the force on every sub-conductor by only considering one sub-conductor per Roebel bar. Since every sub-conductor passes every position inside the Roebel bar once, this estimation process is legitimate. After describing

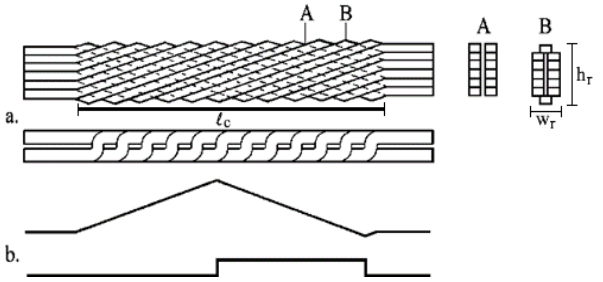

FIGURE 7. Detailed view of a sub-conductor inside a Roebel bar [6].

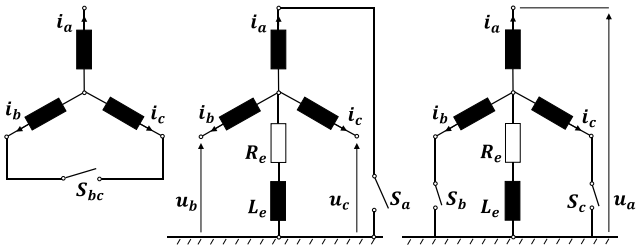

FIGURE 8. Schematic of different asymmetrical short circuits [6].

the origin of the flux densities in the slot, the short-circuit currents and flux densities in the slot are analytically estimated in the subsequent sections.

IV. ANALYTICAL CALCULATION OF SHORT-CIRCUIT CURRENTS

This section gives a brief description about the analytical tool for the calculation of symmetrical and asymmetrical short-circuit currents. The estimation is based on the methods introduced by Hannekam [7]. Figure 8 shows the schematic of different asymmetrical short circuits. In the first step, the three-phase parameters such as voltages, fluxes and currents are transformed to a two-phase system using Park transformation. The voltage equations for stator and rotor circuits are described in equation (7). The superscripts s, r and T refer to the stator and rotor parameter and Park transformation.

$$\begin{bmatrix} v'_s \\ v_R \end{bmatrix} = \begin{bmatrix} T^T \cdot (R_s + R_e) \cdot T & 0 \\ 0 & R_R \end{bmatrix} \begin{bmatrix} i'_s \\ i_R \end{bmatrix} + \frac{d}{dt} \left\{ \begin{bmatrix} T^T \cdot (L_{\sigma s} + L_e + m_{ss}) \cdot T & T^T m_{SR} \\ m_{RS} \cdot T & L_{\sigma R} + M_{RR} \end{bmatrix} \begin{bmatrix} i'_s \\ i_R \end{bmatrix} \right\} \tag{7}$$

The fluxes in the machine stay constant immediately after the short-circuit. Hence, the flux equations can be used to estimate the short circuit currents. In the case of a two-phase short-circuit, the flux equations in two axes coordinates in per unit are given by:

$$\frac{d}{dt} \begin{bmatrix} \psi_\beta \\ \psi_D \\ \psi_Q \\ \psi_F \end{bmatrix} = - \begin{bmatrix} R_S & 0 & 0 & 0 \\ 0 & R_D & 0 & 0 \\ 0 & 0 & R_Q & 0 \\ 0 & 0 & 0 & R_F \end{bmatrix} \begin{bmatrix} i_\beta \\ i_D \\ i_Q \\ i_F \end{bmatrix} + \begin{bmatrix} 0 \\ 0 \\ 0 \\ \hat{E} \cdot (R_F / X_{hd}) \end{bmatrix} \tag{8}$$

The subscript „β“ describes one phase of the two-phase generator, the subscripts „D“ and „Q“ belong to the damper

currents in longitudinal and transverse direction, the subscript „F“ describes the field winding values and $\hat{E}$ is the amplitude of the induced voltage. Assigning zero to the short-circuit voltages, the equation system can be solved. However, to solve this equation set, it should be simplified. This can be done by neglecting the oscillation terms referring to the derivations of the flux after the moment of short circuit. This is reached by integrating the admittances to get the average value of one period (9), as shown at the bottom of the page, „V“ represents the relationships of different reactances and τ is the dimensionless time according to [7]. This equation system can be solved analytically, because it represents equations of order one and one equation of order two. This results in equation (10) with T_β as the stator time constant and T_0 as the moment of short circuit

$$i_\beta = \hat{E} \Big/ m. \left(e^{-\tau / T_\beta} . sin T_0 - h . sin \gamma \right) \tag{10}$$

with $h = h(\tau)$ given by:

$$h(\tau) = \left(1 - \frac{X_d'' + X_v}{X_d' + X_v} \right) e^{-\tau / T_d''} + \left(\frac{X_d'' + X_v}{X_d' + X_v} - \frac{X_d'' + X_v}{X_d + X_v} \right) e^{-\tau / T_d'} \tag{11}$$

It is possible to estimate the short-circuit currents analytically [7]. The comparison between analytical calculations and experimental results for a three-phase sudden short circuit is indicated in Figure 9. The measurement results are obtained from a 220 MVA hydrogenerator with nominal field current of 1600 A.

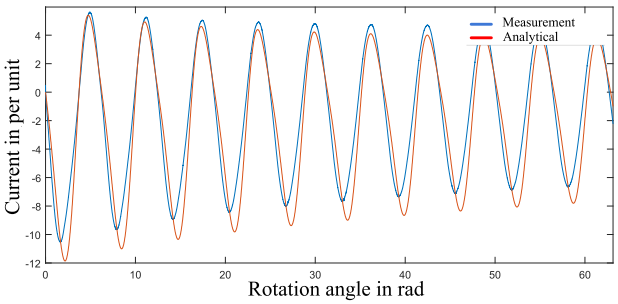

FIGURE 9. Comparison between the analytical calculations and experimental results from a sudden three-phase short circuit of a 220 MVA generator.

V. ANALYTICAL CALCULATION OF RADIAL AND TRANSVERSE FLUXES IN THE SLOT

After the estimation of the short-circuit currents, the slot fluxes need to be calculated analytically. This is described in the next section.

The transverse flux originates partly from the air-gap flux and partly from the conductor bars in the stator. If the permeability of the slot and the teeth is assumed to be constant, the fluxes can be added to obtain the total flux at a given point. An approximation for the estimation of the air gap flux of a salient-pole synchronous machine is given in [8]. With the magnetomotive force $\hat{V}_m(x_r)$, the load angle dependent x_r, it is possible to approximate the flux distribution in the slot with the following empirical equations for the radial flux density $B_{f,x}$ and the transverse flux density $B_{f,y}$

$$B_\delta(x_r) = \frac{\hat{V}_m(x_r)}{\delta(x_r)} \cdot \mu_0 \tag{12}$$

$$B_{f,x}(x, y, x_r) = B_\delta(x_r) \cdot \left(e^{\left(\frac{x \cdot A}{s_h} - B \right)} \cdot \cos\left(\frac{2\pi}{s_\omega} \cdot y \right) \right) \tag{13}$$

$$B_{f,y}(x, y, x_r) = B_\delta(x_r) \cdot \left(e^{\left(\frac{x \cdot A}{s_h} - B \right)} \cdot \sin\left(\frac{2\pi}{s_w} \cdot y \right) + C \cdot \cos\left(\frac{x_r \pi}{\tau_p} \right) \right), \tag{14}$$

where x is the distance from the slot bottom, y is the distance from the slot center to the walls, s_h is the slot height and s_w is the slot width. The starting point is the formulation of flux density distribution in the air gap $B_\delta(x_r)$ [9], [10]. The empirical values in equation 13 and 14 describe the behavior of the flux lines and are influenced by the resistance of the slot teeth and slot area. These values are originally approximated with the least square method from FEM results in rated operation to resemble the common behavior of the flux lines without knowing the exact magnetic resistance of the magnetic circuit. These values are also assumed to be unchanged during the short circuit. These equations consider

$$\frac{d}{d\tau} \begin{bmatrix} \psi_\beta \\ \psi_D \\ \psi_Q \\ \psi_F \end{bmatrix} = -\frac{1}{X_d'' + V_{C1}'' \cdot X_q''} \cdot \begin{bmatrix} R_S \cdot (1 + V_A'') & 0 & 0 & 0 \\ 0 & R_D (V_{DD} + V_{C1}'' + V_{qD}) & 0 & -R_D . (V_{DF} + V_{C1}'' + V_{qh}) \\ 0 & 0 & R_Q (V_{dQ} + V_{C1}'' + V_{QQ}) & 0 \\ 0 & R_F (V_{DF} + V_{C1}'' + V_{qh}) & 0 & R_F (V_{FF} + V_{C1}'' + V_{qF}) \end{bmatrix} \cdot \begin{bmatrix} \psi_\beta \\ \psi_D \\ \psi_Q \\ \psi_F \end{bmatrix} + \begin{bmatrix} 0 \\ 0 \\ 0 \\ \hat{E} . (R_F / X_{hd}) \end{bmatrix} \tag{9}$$

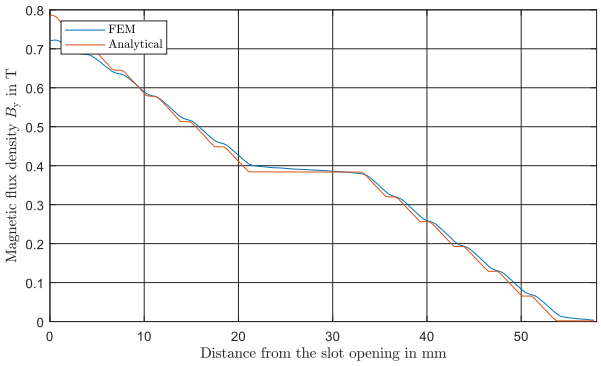

FIGURE 10. Result of the calculation of the flux distribution inside the slot center.

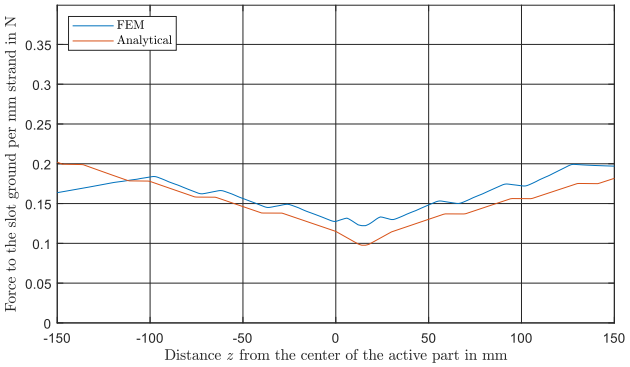

FIGURE 11. Forces per mm on a sub-conductor in a Roebel bar.

together with the empirical values A = 10.2, B = 9.7 and C = 0.02, the decrease of flux density in the slot area resulting from the bending of the flux lines into the slot walls and also the bending itself. The last cosine function is related to the load angle dependent flux through the slot. Together with the flux density originated from the stator winding $B_{c,y}$, described in section B, this results in the total flux density in the slot at any point:

$$B_y(x, y, x_r) = B_{c,y}(x) + B_{f,y}(x, y, x_r) \tag{15}$$

$$B_x(x, y, x_r) = B_{f,x}(x, y, x_r) \tag{16}$$

The calculation results for a slot of a salient-pole machine at rated power are shown in Figure 10. The flux density near the slot ground is mainly influenced by the current in the sub-conductors and therefore results in an evenly step-shaped distribution. However, the closer the viewing point gets to the rotor, the more the flux density is influenced by the rotor. This results in a bending in the graph at the slot opening.

VI. ANALYTICAL CALCULATION OF ROEBEL BAR FORCES CONSIDERING TRANSPOSITION

To calculate the forces on the sub-conductors, the formulation of the lorentz force on a current-carrying wire is used [11], [12]

$$\vec{F}_L = \boldsymbol{I} \int \mathrm{d}\vec{l} \times \vec{B} \tag{17}$$

To consider the changing flux density in every sub-conductor, the mean value of the flux density in the area of the sub-conductor is calculated. If it is assumed that the flux over the length of the active part is constant, the length of the conductor rod can be integrated to get the force on the whole sub-conductor. To consider the transposition of the sub-conductors in the slot at any given depth, the geometry of the stator core and the conductors must be known. As the geometry of a Roebel bar is relatively complex, it is assumed that every sub-conductor starts at a given position in the Roebel bar when entering the active part of the generator, leaves it at the same position and the current of every sub-conductor is constant. Furthermore, every sub-conductor inside the active part reassembles one period of a triangle function in radial direction and a square wave functional in transverse direction (Figure 7-b), so that an analytical approximation of the path is possible. Finally, the sub-conductor is separated in evenly sized parts and the flux passing every part is calculated by using the resulting geometrical functions and assuming a constant flux over the conducting cross section of the sub-conductor.

$$\Delta x(z) = h_r \cdot \left| \mathrm{mod}\left(1 - \left(\frac{2}{l_c} \cdot \left(z - k_{sc} \cdot \frac{l_c}{n_{sc}}\right)\right), 2\right) - 1 \right| - \frac{h_r}{2} \tag{18}$$

$$\Delta y(z) = \left(\mathrm{rect}\left(\left(\frac{z}{l_c} - \frac{k_{sc}}{n_{sc}}\right) - 0,5\right)\right) \cdot \frac{w_r}{2} \tag{19}$$

With the geometrical dimension of the Roebel bar, this leads to the equations (18) for the radial direction and (19) for the transverse direction, where l_c is the active part length, h_r is the maximum height of the Roebel bar, w_r is the maximum width, n_{sc} is the number of sub-conductors per Roebel bar and k_{sc} is the chosen bar from 1 to $\boldsymbol{n}_{sc}$ (Figure 7), resulting in an offset of the sub-conductors from the geometrical center of the Roebel bars. When this is used in conjunction with equations for the flux originated from the stator and rotor, it is possible to calculate the force on every sub-conductor in a Roebel bar with known dimensions as shown in Figure 11.

To validate the calculated results, the FEM Programs (ANSYS, Opera and FEMM) are used. The 3D FEM calculations are carried out using Opera 3D. The air gap vector potential values are then transformed into an FEMM 2D model for a detailed modelling of the sub-conductors of the Roebel bar. The numerical validation of the short-circuit calculation is done with ANSYS. Also a one-pole model of the generator is simulated with FEMM which is indicated in Figure 2-a. The calculations are carried out for an under-scaled hydrogenerator shown in Figure 2-b. It is a 16 pole salient-pole generator with 96 slots, a double-layer fractional slot winding with 12 sub-conductors per Roebel bar (Figure 2-b). The nominal field current is 260 A and the stator current the 1200 A. On the test computer, the FEM simulation required approximately 287 seconds for a single solution of the problem, while the analytical calculation was done in less than 20 milliseconds.

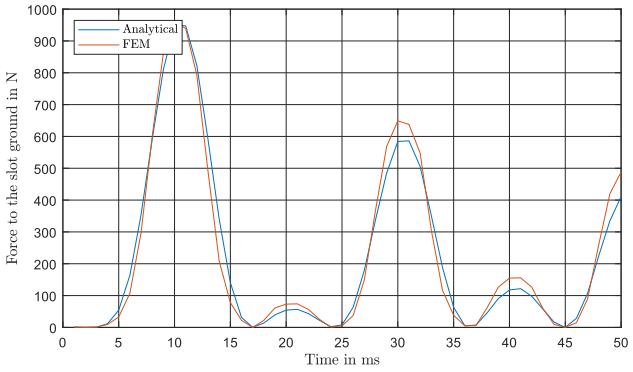

FIGURE 12. Comparison between the total calculated forces against the slot ground on a sub-conductor in a Roebel bar.

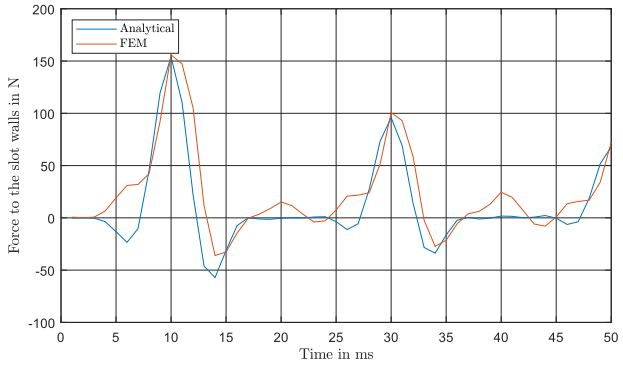

FIGURE 13. Comparison between the total calculated forces against the slot walls on a sub-conductor in a Roebel bar.

VII. ESTIMATION OF ROEBEL BAR FORCES AT SHORT CIRCUIT

With the described methods and equations, it is now possible to estimate the force on Roebel bar sub-conductors in case of a short circuit. The calculated currents over time are used as input for the calculation of the flux density in the slot with the equations (12) to (16).

With the known current in the sub-conductor, a constant load angle, the equations (18) and (19) and the position of the transposed sub-conductors, the forces on the sub-conductors can be calculated by:

$$\vec{\boldsymbol{B}}\left(\boldsymbol{x},\boldsymbol{y},\boldsymbol{x_r}\right) = \begin{pmatrix} \boldsymbol{B_x}\left(\boldsymbol{x},\boldsymbol{y},\boldsymbol{x_r}\right) \\ \boldsymbol{B_y}\left(\boldsymbol{x},\boldsymbol{y},\boldsymbol{x_r}\right) \\ \boldsymbol{0} \end{pmatrix} \tag{20}$$

$$\overrightarrow{\boldsymbol{F_r}}\left(\boldsymbol{I},\boldsymbol{x_r}\right) = \boldsymbol{I}\int_0^{l_c} \vec{\boldsymbol{e}}_z \times \vec{\boldsymbol{B}}\left(\boldsymbol{x_s} + \boldsymbol{\Delta x}\left(z\right), \boldsymbol{y_s} + \boldsymbol{\Delta y}\left(z\right), \boldsymbol{x_r}\right) \mathrm{d}z, \tag{21}$$

where $\boldsymbol{x_s}$ is the distance of the center of the Roebel bar from the rotor pole shoe surface and $\boldsymbol{y_s}$ is the offset of the Roebel bar from the center of the slot, in most cases $\boldsymbol{y_s} = 0$. The graphs in Figures 12 and 13 compare the analytical calculation using equation (21) and FEM simulation. The deviation of the two plots mainly results from assuming a constant permeability of the teeth and the slot. In a real generator, the teeth are saturated in case of a short circuit and therefore the permeability of the teeth is less than in rated operation.

On the one hand, this leads to more flux entering the slot from the slot opening resulting in a larger B_x and therefore in a larger force against the slot walls in the simulated results in Figure 12. On the other hand, the saturated teeth result in a different ratio between the permeability of the teeth and the stator yoke, resulting in less flux passing the slot and therefore in a smaller B_y in the slot than calculated. Another point worth noting is that because of the transposition of the sub-conductors, the direction of the infinitesimal length is not strictly aligned in the axial direction (z-axis) of the core. This will add a small force f_z in axial direction. That axial force is only approx. 2% as strong as the force against the slot ground per sub-conductor and gets mostly nullified by adding the force on all sub-conductors together and is therefore neglected.

VIII. DISCUSSIONS

In general, the magnetic forces on the Roebel bar are predominantly in the radial direction and cause cyclic compression of the main insulation against the slot bottom. Nevertheless, this work shows that the radial field component coming from the air gap contributes in generating forces in tangential direction. This lateral force is normally disregarded in literature, but may cause significant cyclic compression of the main insulation against the slot side wall during the short circuit, since the Roebel bar forces during the short circuits are up to 250 times bigger than during normal operation. Depending on the tightness of the bars inside the slot, a combination of these radial and tangential forces may also induce relative movement between bars and core lamination.

The discrepancies between the calculated and the simulated results are mainly caused by the sinusoidal approximation of the air gap flux density over the pole shoe in the analytical model. In reality, there are damper windings and saturation effects in the pole shoe which are neglected here. Furthermore, the saturation of the teeth near the slot opening is neglected which results in more flux passing through the slot opening in case of a short circuit and therefore results into a larger simulated flux density than the calculated one. This can be particularly observed in Figure 13, where the flux density of the simulation is positive before the peak, while the calculated results are negative. In this case, the approximation of a sinusoidal flux does not fit well, because the saturation effects in the pole shoe and the teeth force the flux into the opposite direction than anticipated. This can be improved by adding a model of the magnetic resistance to the calculation which would significantly increase the complexity of the calculation.

Another decisive step is to calculate the stress on the Roebel bar insulation and fixation components. In literature [2], [3], a mechanical calculation of the bar inside the slot is performed. Different mechanical boundary conditions are considered, showing the impact of having a tight or a loose bar fixation system. However, only the static condition was assessed and only the magnetic forces on the conductors were considered. The dynamic behavior of the bars inside

the slot is not discussed in detail in existing literature, and the effect of inertia forces due to the stator core vibration is commonly not considered. Future investigations should be done to model these dynamic effects, considering the alternating magnetic forces on the conductors, the core laminations, global vibration and the mechanical response of the insulation system. Thereby, it is expected that the calculated mechanical stresses can serve as inputs for the stress ageing model of the insulation system.

IX. CONCLUSION

In this paper, an analytical model for the comprehensive calculation of radial and tangential Roebel bar forces during short circuits is presented. Besides the development of analytical models for estimation of asymmetrical short circuits, analytical methods for calculating the radial and tangential fluxes in the slot are introduced. Beyond the state of the art, the influence of rotor dynamics on radial and tangential slot fluxes is considered. Based on the calculated fluxes and currents, the forces on each sub-conductor in the Roebel bar can be determined. Since the sub-conductors are transposed in the longitudinal direction of the machine, mathematical models for considering these three-dimensional transpositions are developed. With the model developed in this paper, it is possible to analytically estimate the Roebel bar forces during symmetrical and asymmetrical short circuits.

REFERENCES

[1] A. Ebrahimi, "Characterization of a large electrical machine test bench for advanced investigations on wind and hydro generators," in *Proc. IEEE 4th Southern Power Electron. Conf. (SPEC)*, Singapore, Dec. 2018, pp. 1–6.

[2] C. Grabner and E. Schmidt, "Analytical approximation of the displacement process of Roebel bars," in *Proc. Conf. Rec. IEEE Ind. Appl. Conf. 37th IAS Annu. Meeting*, Feb. 2002, pp. 1135–1141.

[3] C. Grabner and H. Köfler, "Mechanical stress behavior inside slots of large hydro generators," in *Proc. Int. Conf. Renew. Energy Power Qual.*, 2003, pp. 1–8, doi: 10.24084/repqj01.313.

[4] M. G. Pantelyat, O. Biro, and A. Stermecki, "Electromagnetic forces in synchronous turbogenerator rotor slot wedges," in *Proc. Joint INDS ISTET*, Klagenfurt, Austria, Jul. 2011, pp. 1–4.

[5] J. Pyrhönen, *Design of Rotating Electrical Machines*. Hoboken, NJ, USA: Wiley, 2013.

[6] T. Dordea, V. Muller, I. Torac, G. Madescu, M. Moţ, and L. Ocolişan, "Analytical method for the optimization of Roebel bars composed of full elementary conductors," Romanian Academy, Bucharest, Romania, Tech. Rep., Jan. 2006. [Online]. Available: https://www.researchgate.net/publication/228994422_Analytical_method_for_the_optimization_of_Roebel_bars_composed_of_full_elementary_conductors

[7] L. Hannekam, "Entwicklung geschlossener Nähreungen für symmetrische Stosskurzschlüsse der synchronen Schenkelpolmaschine," in *Archiv dür Elektrotechnik, Band 45, Heft 2*. New York, NY, USA: Springer-Verlag, 1960.

[8] A. Binder, *Elektrische Maschinen und Antriebe*, E. P. Wigner, Ed. Berlin, Germany: Springer-Verlag, 2012.

[9] B. Sanosian, P. Wendling, T. Pham, and W. Akaishi, "Electromagnetic forces on coils and bars inside the slot of hydro-generator," in *Proc. IEEE Energy Convers. Congr. Expo. (ECCE)*, Baltimore, MD, USA, Sep. 2019, pp. 1754–1760.

[10] A. C. Viorel, I.-A. Viorel, and L. Strete, "On the calculation of the carter factor in the slotted electric machines," in *Proc. Int. Conf. Expo. Electr. Power Eng. (EPE)*, Romania, Balkans, Oct. 2014, pp. 332–336.

[11] A. E. Fitzgerald, C. Klingley, S. D. Umans, and B. James, *Electric Machinery*. New York, NY, USA: McGraw-Hill, 2003.

[12] C. Grabner, "Comparative study on the analytical and numerical calculation of no-load harmonics in large salient-pole synchronous machines," in *Proc. Int. Symp. Power Electron., Electr. Drives, Autom. Motion*, Taormina, Italy, May 2006, pp. 390–395.

MARIUS WENZEL MEISWINKEL received the B.Sc. degree in electrical engineering from Leibniz University Hannover, Germany, in 2019, where he is currently pursuing the M.Sc. degree in electrical engineering.

He is currently working as a Student Research Assistant with the Institute for Drive Systems and Power Electronics, Hannover. His works include the enhancement and further development of simulation software and research in the analytical calculation of slot fields and forces on stator bars in case of short circuits to enhance the understanding of the mechanical behavior and failure prediction in large hydrogenerators.

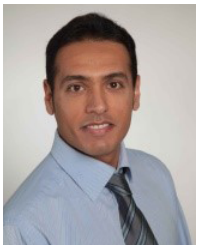

AMIR EBRAHIMI received the B.Sc. degree from Shiraz University, in 2006, the M.Sc. degree in electrical engineering from the Iran University of Science and Technology, in 2008, and the Ph.D. degree in electrical engineering from the University of Stuttgart, Germany, with a dissertation on "Analytical modeling and optimization of surface mounted permanent magnetic synchronous motors considering spatial harmonics." From 2013 to 2017, he was with the Fraunhofer Institute for Manufacturing Engineering and Automation, Stuttgart. He was the Group Manager for drive systems and exoskeletons and developed among others, the first European upper body exoskeletons. Since November 2017, he has been a Professor in Electrical Machines with the Institute for Drive Systems and Power Electronics, Leibniz University Hannover. His research interests include the analytical and numerical calculation of transient processes in electrical machines, particularly in large hydro and wind generators. He is a member of the European Energy Research Alliance and Wind Research center. He is a Reviewer of the IEEE TRANSACTIONS ON INDUSTRIAL ELECTRONICS and other journals, and an author and editor of the book "*Advances on analytical modelling of hydro and wind generators*."

CONSTANTIN WOHLERS was born in Gehrden, Germany, in August 1990. He received the master's degree in industrial engineering from Leibniz University Hannover, in 2015. Since 2015, he has been working as a Research Associate with the Institute for Drive Systems and Power Electronics. His research interests include analytical modeling of permanent magnet synchronous machines and design of high torque motors. His master thesis was awarded with the Ernst-Blickle Graduate Award, in 2015.

TIM NESCHITSCH received the B.Sc. degree in electrical engineering from the Leibniz University Hannover, Germany, in 2019, where he is currently pursuing the M.Sc. degree in electrical engineering.

During his bachelor thesis about analytical short-circuit currents in synchronous machines, he designed a simulation software to calculate, draw, and export symmetric and asymmetric short circuit-currents. He is also working as a Student Research Assistant with the Institute for Drive Systems and Power Electronics, Leibniz University Hannover, to continue his work on short-circuit current calculations.